JOURNAL OF AIRCRAFT
Vol. 31, No. 3, May–June 1994

Significance of the Dihedral Effect in Rapid Fuselage-Reorientation Maneuvers

Spiro Bocvarov,* Eugene M. Cliff,† and Frederick H. Lutze‡
Virginia Polytechnic Institute and State University, Blacksburg, Virginia 24061

A study is presented about the role the dihedral effect (rolling moment due to sideslip) can have in fuselage-reorientation maneuvers that involve high angles of attack. A mathematical model for attitude maneuvers is developed, which accurately represents the High Angle-of-Attack Research Vehicle, including propulsive moments generated by thrust-vectoring. The fuselage-reorientation problem is posed as an unconstrained time-optimal control problem, and numerical extremal trajectories are obtained. These trajectories are examined in order to determine if and when the dihedral effect contributes significantly to the maneuvers. Results indicate that for most reorientation maneuvers the dihedral effect is small, and that these minimum-time trajectories occur with small sideslip angles.

I. Introduction

VARIOUS technological advances have enabled the development of a new generation of combat aircraft, with expanded flight envelope and improved maneuvering capabilities (supermaneuverable aircraft[1–4]). These aircraft will be more "agile" and have the ability to operate at extreme angles of attack. One of the enabling technologies is the concept of propulsive control-moments,[5,6] generated by thrust-vectoring (TV). At higher angles of attack, where the aerodynamic control surfaces are less effective, TV can be used for attitude control, while at lower angles of attack the propulsive control-moments can supplement the aerodynamic control surfaces.

In order to gain a tactical advantage in a combat situation, it is desirable to perform the combat maneuvers in minimum time. Modern computers and advanced numerical techniques, along with the accurate aircraft aerodynamic models obtained from wind-tunnel measurements, facilitate numerical study of the problem of optimal tactical maneuvering. The authors have recently reported[7,8] an analytical mathematical model for the High Angle-of-Attack Research Vehicle[9] (HARV), developed for study of time-optimal fuselage-reorientation maneuvering problems. The model neglects the translational motion of the aircraft (therefore being valid only for rapid attitude maneuvers, during which the aircraft velocity-vector does not change significantly). Results obtained with this model can be used as a starting point for a 6-degree-of-freedom model and more complex tactical-maneuvering optimal control problems.

In performing minimum-time reorientation maneuvers, one might expect that the use of sideslip to create rolling moment (dihedral effect) might be a useful means to reduce the maneuvering time. In this article we look at this possibility in detail, and show that for a large class of reorientation maneuvers of practical interest and tactical significance the dihedral effect appears to have little influence upon maneuvering time. However, there are maneuvering problems in which the dihedral effect can be utilized with some benefit. The distinctions between these classes of maneuvers is important in the design of flight-test evaluation procedures.

The mathematical model is described in Sec. II. Control variables are the actual deflections of the aerodynamic control surfaces and the thrust-vectoring system. Particular emphasis is put upon the structure of the dynamical equations, since most of the analysis is based upon understanding the role of various dynamical components and their mutual tradeoffs in the course of the extremal trajectories.

In Sec. III we briefly show how the time-optimal, fuselage-reorientation problems are defined as optimal control problems, and how candidate solutions of a problem are characterized by the minimum principle.[10–12] We restrict our attention to the class of reorientation maneuvers that have zero angular rates at the initial and final point (rest-to-rest maneuvers).

Section IV presents results obtained in a few parametric studies, for rest-to-rest maneuvers with zero sideslip-angle at the endpoints. Two families of extremal maneuvers, involving angles of attack up to 60 deg, are examined. The benefit, and in some cases the adverse effect, of the dihedral moment in the course of the extremal maneuvers is discussed and supplemented by a few plots.

In certain situations, such as when one wants to lock and fire on a target, it is necessary that the aircraft weapons (and radar system) are pointed properly, but it is not necessary for the aircraft sideslip-angle to be zero. A case study is presented in Sec. V, which shows how the dihedral effect can be advantageously utilized in maneuvering time improvement for certain maneuvers of this type.

In Sec. VI we explain certain general features of the extremal solutions discussed, in an attempt to elucidate why these maneuvers exhibit low sideslip-angles (the time-optimal control problems were posed as unconstrained optimization problems). From a purely mathematical perspective, we try to understand how the $C_l^0(\alpha, \beta)$ dynamical component in the mathematical model [Eq. (5)] affects the optimization process.

II. Attitude-Maneuvering Model

In the development of a mathematical model for time-optimal fuselage-reorientation maneuvers, we restrict our interest to low values of dynamic pressure. Rapid attitude-maneuvers at higher dynamic pressure are undesirable since the accelerations the aircraft then undergoes are unacceptable for

Received June 10, 1992; presented as Paper 92-4490 at the AIAA Atmospheric Flight Mechanics Conference, Hilton Head, SC, Aug. 10–12, 1992; revision received Feb. 24, 1993; accepted for publication April 23, 1993.

*Research Associate, Aerospace and Ocean Engineering Department. Member AIAA.
†Reynolds Metals Professor, Aerospace and Ocean Engineering Department. Associate Fellow AIAA.
‡Professor, Aerospace and Ocean Engineering Department. Associate Fellow AIAA.

the human pilot. At moderate altitudes (say, $h \approx 15{,}000$ ft) and low Mach numbers ($M < 0.4$), the velocity-vector of the aircraft does not change significantly in the course of a rapid fuselage-reorientation maneuver. The motions of interest are fast enough (say, on the order of 2 or 3 s) so that we can assume that linear displacements of the aircraft c.m. from the line of the original direction and changes in Mach number and dynamic pressure are small. These assumptions allow us to neglect the linear motion of the aircraft and analyze only the angular motion in the course of the fuselage-reorientation maneuvers. Thus, a 3-degree-of-freedom mathematical model is quite relevant for our studies. One can visualize the aircraft in a wind tunnel, free to rotate about the c.m. We are essentially interested in how the aerodynamic control surfaces (and the TV system) can be utilized most effectively, so as to reorient the aircraft from one attitude to another in minimum time.

It is assumed that there is no aircraft mass change in amount and distribution in the course of the fuselage-reorientation maneuvers. For the present study we have neglected the effects of the flaps and the speed brake. What follows is a brief derivation of the mathematical model.

A. Kinematical Relations

Based upon the assumption of a model with "fixed" c.m., it is possible to devise a set of angles α (the angle of attack), β (the sideslip-angle), and μ (the wind-axes roll angle), that can describe the attitude of the aircraft uniquely, almost everywhere.[13,14] Also, because of our assumptions, the angular velocity of the wind reference frame with respect to the local horizontal frame ($\bar{\omega}^w$) has a nonzero component only along its x_w axis ($q_w = r_w = 0$).

Let us assume that at initial time, prior to the beginning of a maneuver, the wind reference frame coincides with the local horizontal reference frame. This situation may correspond, e.g., to a steady-state level flight. As the aircraft starts maneuvering and $\bar{\omega}^w \neq 0$, the relative position of the wind reference frame with respect to the local horizontal reference frame is uniquely specified by a roll angle μ, the angular rate being $p_w = d\mu/dt$. The aerodynamic angles α and β specify uniquely the orientation of the aircraft body-fixed reference frame with respect to the wind reference frame.

The (relative) angular velocity of the body-fixed reference frame with respect to the wind reference frame[13] is given by

$$\bar{\omega}^{\text{rel}} = \bar{\omega}^b - \bar{\omega}^w = -\hat{k}^w \frac{d\beta}{dt} + \hat{j}^b \frac{d\alpha}{dt} \tag{1}$$

From Eq. (1) we derive the kinematical equations [Eq. (6)].

B. Angular-Rate Dynamics

The aircraft is assumed rigid body. The Euler rigid-body rotational equations[13,15] are given by the following set of differential equations:

$$\begin{aligned} I_x \frac{dp}{dt} &= (I_y - I_z)qr + u_x + \frac{1}{2}\rho V^2 S b C_l \\ I_y \frac{dq}{dt} &= (I_z - I_x)rp + u_y + \frac{1}{2}\rho V^2 S \bar{c} C_m \\ I_z \frac{dr}{dt} &= (I_x - I_y)pq + u_z + \frac{1}{2}\rho V^2 S b C_n \end{aligned} \tag{2}$$

In the above expressions, u_x, u_y, and u_z denote the propulsive moments, generated by thrust-vectoring. Besides the propulsive moments, the rigid-body dynamics depends upon the dynamic pressure $\bar{q} = \rho V^2/2$ (which is a function of the altitude h and the Mach number M), and upon the aerodynamic controls and the aerodynamic angles α and β (expressed through the aerodynamic moment-coefficients C_l, C_m, and C_n).

The current implementations of the thrust vectoring system can be plausibly modeled in the following way (u_x^0, u_y^0, and u_z^0 are constants):

$$\begin{aligned} u_x(\delta_x) &= u_x^0 \delta_x \\ u_y(\delta_y) &= u_y^0 \delta_y \\ u_z(\delta_z) &= u_z^0 \delta_z \end{aligned} \tag{3a}$$

$$|\delta_x|^n + |\delta_y|^n + |\delta_z|^n \leq 1.0 \tag{3b}$$

It is convenient to use $n = 2$, which gives a reasonable model for thrust-vectoring, and is also a nice choice for analytical reasons.

The aerodynamic moments are very complex functions, each depending upon the angles α and β (see Fig. 1) as well as the Mach number, altitude, and deflections of all of the aerodynamic control surfaces (cross-coupling effects). However, many of these dependencies can be neglected for the problem considered. The Mach number and the dynamic pressure are assumed constant throughout the maneuvers.

It is assumed that only "conventional" aerodynamic controls will be used, each control affecting a single axis: the ailerons are used in differential manner for roll control, the rudders for yaw control, and the horizontal tails for pitch control (as an elevator) only. It is assumed that there are three primary controls (Δ_a^*, δ_e^*, and δ_r^*) such that

$$\begin{aligned} \delta_a^r &= -\delta_a^l = \Delta_a^* \\ \delta_e^r &= +\delta_e^l = \delta_e^* \\ \delta_r^r &= +\delta_r^l = \delta_r^* \end{aligned} \tag{4}$$

where superscripts r and l refer to left and right surface, respectively.

Under these circumstances and assumptions, an accurate representation of the aerodynamic moments and control-surface effectiveness is obtained if the following functional dependencies are assumed:

$$C_l = C_l^0(\alpha, \beta) + C_l^\zeta(\alpha, p) + C_l^c(\alpha, \Delta_a^*) \tag{5a}$$

$$C_m = C_m^0(\alpha, \beta) + C_m^\zeta(\alpha, q) + C_m^c(\alpha, \delta_e^*) \tag{5b}$$

$$C_n = C_n^0(\alpha, \beta) + C_n^\zeta(\alpha, r) + C_n^c(\alpha, \delta_r^*) \tag{5c}$$

Here, C_i^0, C_i^ζ, and C_i^c ($i \in \{l, m, n\}$) denote the rigid-body static (all control surfaces in neutral position), rate damping,

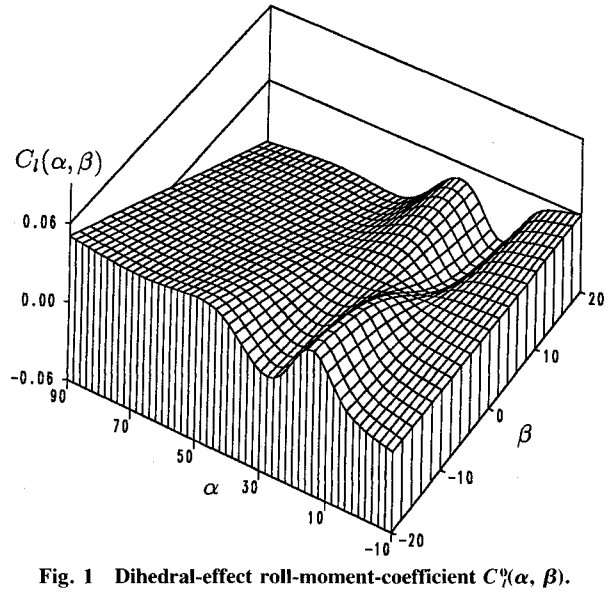

Fig. 1 Dihedral-effect roll-moment-coefficient $C_l^0(\alpha, \beta)$.

and aerodynamic control surface contributions to the aerodynamic moment coefficients, respectively.

Analytic models were constructed for the aerodynamic functions in Eq. (5) using data from the HARV data base for the range of $\alpha \in (-10 \text{ deg}, +90 \text{ deg})$ and $\beta \in (-20 \text{ deg}, +20 \text{ deg})$. These analytic models fit the data available with less than 5% error for angles of attack less than 75 deg. Certain cross-coupling effects are neglected [see Eq. (5)]. The model used in obtaining numerical results corresponds to $M = 0.3$ and $h = 15{,}000$ ft.

C. Scaled Mathematical Model

The mathematical model was scaled for numerical reasons. The complete, scaled mathematical model is:

$$\dot{\alpha} \equiv \frac{d\alpha}{d\tau} = Q - (P \cos\alpha + R \sin\alpha)\tan\beta \tag{6a}$$

$$\dot{\beta} \equiv \frac{d\beta}{d\tau} = P \sin\alpha - R \cos\alpha \tag{6b}$$

$$\dot{\mu} \equiv \frac{d\mu}{d\tau} = (P \cos\alpha + R \sin\alpha)\frac{1}{\cos\beta} \tag{6c}$$

$$\dot{P} = \underbrace{\varepsilon_t J_{sx} a_x \delta_x}_{L_t} + \underbrace{\varepsilon_{\bar{q}} J_{sx} B_s C_l(\cdot)}_{L_a} + \underbrace{J_x QR}_{L_{qr}} \tag{7a}$$

$$\dot{Q} = \underbrace{\varepsilon_t J_{sy} a_y \delta_y}_{M_t} + \underbrace{\varepsilon_{\bar{q}} J_{sy} C_s C_m(\cdot)}_{M_a} + \underbrace{J_y RP}_{M_{rp}} \tag{7b}$$

$$\dot{R} = \underbrace{\varepsilon_t J_{sz} a_z \delta_z}_{N_t} + \underbrace{\varepsilon_{\bar{q}} J_{sz} B_s C_n(\cdot)}_{N_a} + \underbrace{J_z PQ}_{N_{pq}} \tag{7c}$$

where (abbreviating $\mathcal{L} = \varepsilon_{\bar{q}} J_{sx} B_s$, $\mathcal{M} = \varepsilon_{\bar{q}} J_{sy} B_s$, and $\mathcal{N} = \varepsilon_{\bar{q}} J_{sz} B_s$)

$$L_a = \underbrace{\varepsilon_l^0 \mathcal{L} C_l^0}_{L_0} + \underbrace{\varepsilon_\zeta \mathcal{L} C_l^\zeta}_{L_\zeta} + \underbrace{\varepsilon_a \mathcal{L} A(\alpha)\Delta_a}_{L_c} \tag{8a}$$

$$M_a = \underbrace{\varepsilon_m^0 \mathcal{M} C_m^0}_{M_0} + \underbrace{\varepsilon_\zeta \mathcal{M} C_m^\zeta}_{M_\zeta} + \underbrace{\varepsilon_e \mathcal{M} E(\alpha, \delta_e)}_{M_c} \tag{8b}$$

$$N_a = \underbrace{\varepsilon_n^0 \mathcal{N} C_n^0}_{N_0} + \underbrace{\varepsilon_\zeta \mathcal{N} C_n^\zeta}_{N_\zeta} + \underbrace{\varepsilon_r \mathcal{N} R(\alpha)\,\delta_r}_{N_c} \tag{8c}$$

[compare to Eq. (5)], and

$$E(\alpha, \delta_e) = F(\alpha)\delta_e + G(\alpha) \tag{9}$$

In the above $\tau_{\text{scaled}} = kt$, $(P, Q, R) = (p/k, q/k, r/k)$, $k = \sqrt{u_s^0/l_s}$, l_s, and u_s^0 are scaling constants; J_x, J_y, J_z, B, B_s, C, C_s, J_{sx}, J_{sy}, J_{sz}, a_x, a_y, and a_z are related to the aircraft design parameters and flight conditions.

Note that the aerodynamic control terms modeled by Eqs. (8) and (9) display linear dependence on the scaled control variables. While this appears to be a severe restriction of the more general expression (5), it is not quite so. As stated below, in Sec. III, the maximum principle requires that the controls Δ_a^*, δ_e^*, and δ_r^* in Eqs. (5a–5c) be used in such a manner that maximal power is exerted in the roll, pitch, and yaw channel (7a–7c), in the course of a regular extremal trajectory. Consider now, e.g., the aerodynamic roll control term in Eq. (5a). For each fixed α one can define $A(\alpha) = \max\{C_l(\alpha, \Delta_a^*)\}$ for $\Delta_a^* \in [\Delta_a^{\min}, \Delta_a^{\max}]$. Thus, the scaled control variable [Eq. (8a)] can be interpreted as a fraction of the maximum available aerodynamic roll power. Similar interpretations apply to the pitch and yaw controls. Now that the scaled aerodynamic controls appear linearly, regular extremals will exhibit bang-bang bahavior. This justifies the use of linear controls in the scaled model. This was done primarily for convenience in the numerical (algorithmic) minimization[7,16] of the variational Hamiltonian.

The scaling parameters ε_t, $\varepsilon_{\bar{q}}$, ε_ζ, ε_a, ε_e, ε_r, ε_l^0, ε_m^0, and ε_n^0 will be referred to as homotopy variables; the mathematical model represents the physical system of interest (the HARV) when each of the homotopy variables has a unit value. When $\varepsilon_t = 0$, the mathematical model represents a vehicle with no thrust-vectoring capability.

Considerations of the qualitative and quantitative characteristics of the aerodynamic moment coefficients are an integral part of the analysis of the extremal solutions. However, it is not possible to display all of the figures in the present article. Only $C_l^0(\alpha, \beta)$ is shown, in Fig. 1. For more detailed discussion about the mathematical model, the reader is referred to Refs. 7 and 8.

III. Optimal Control Problem Formulation

A. Boundary Conditions and Cost Function

We want to guide the system from a given initial state to a given terminal state in minimum time. We consider a class of maneuvers which can be characterized by

$$x_0 = [\alpha(t_0), \beta(t_0), \mu(t_0), P(t_0), Q(t_0), R(t_0)]^T = (\alpha_0, \beta_0, \mu_0, 0, 0, 0)^T \tag{10a}$$

$$x_f = [\alpha(t_f), \beta(t_f), \mu(t_f), P(t_f), Q(t_f), R(t_f)]^T = \alpha(t_f, \beta_f, \mu_f, 0, 0, 0)^T \tag{10b}$$

The cost function here is

$$J = \int_{t_0}^{t_f} f^0[x(t), u(t)]\,dt = \int_{t_0}^{t_f} 1\,dt = t_f - t_0 \tag{11}$$

These define the class of minimum-time, rest-to-rest reorientation maneuvers.

B. Adjoint Variables and Optimality Conditions

The dynamics of the adjoint variables λ_α, λ_β, λ_μ, λ_P, λ_Q, and λ_R are given by the following set of differential equations[10–12]:

$$\frac{d\lambda_\nu}{\partial t} = -\frac{\partial H}{\partial \nu}, \qquad \nu \in (\alpha, \beta, \mu, P, Q, R) \tag{12}$$

where

$$H = H(\lambda, x, u) = \lambda^0 f^0 + \sum_\nu \lambda_\nu \dot{\nu}(x, u) \tag{13}$$

is the variational Hamiltonian of the system.

C. Optimality Conditions

Normality[11,12] of the problem is assumed ($\lambda^0 = +1 > 0$). Only the following part of the Hamiltonian depends upon the control vector $\boldsymbol{u}(t) = (\delta_x, \delta_y, \delta_z, \Delta_a, \delta_e, \delta_r)^T$:

$$\begin{aligned} H^c = {} & + \lambda_P[\varepsilon_t J_{sx} a_x \delta_x + \varepsilon_{\bar{q}} \varepsilon_a J_{sx} B_s A(\alpha)\Delta_a] \\ & + \lambda_Q[\varepsilon_t J_{sy} a_y \delta_y + \varepsilon_{\bar{q}} \varepsilon_e J_{sy} C_s F(\alpha)\delta_e] \\ & + \lambda_R[\varepsilon_t J_{sz} a_z \delta_z + \varepsilon_{\bar{q}} \varepsilon_r J_{sz} B_s R(\alpha)\delta_r] \end{aligned} \tag{14}$$

The extremal TV controls are computed from

$$\delta_x = -(\lambda_P J_{sx} a_x)/D \tag{15a}$$

$$\delta_y = -(\lambda_Q J_{sy} a_y)/D \tag{15b}$$

$$\delta_z = -(\lambda_R J_{sz} a_z)/D \tag{15c}$$

where $D = \sqrt{(\lambda_P J_{sx} a_x)^2 + (\lambda_Q J_{sy} a_y)^2 + (\lambda_R J_{sz} a_z)^2}$. The aerodynamic controls appear linearly in the system dynamics and are independent. When λ_P, λ_Q, and λ_R are not equal to zero, the optimality condition[10-12] yields

$$\Delta_a = -\text{sgn}[\lambda_P \varepsilon_{\bar{q}} \varepsilon_a J_{sx} B_x A(\alpha)] \equiv -\text{sgn}(\lambda_P) \tag{16a}$$

$$\delta_e = -\text{sgn}[\lambda_Q \varepsilon_{\bar{q}} \varepsilon_e J_{sy} C_x F(\alpha)] \equiv -\text{sgn}(\lambda_Q) \tag{16b}$$

$$\delta_r = -\text{sgn}[\lambda_R \varepsilon_{\bar{q}} \varepsilon_r J_{sz} B_x R(\alpha)] \equiv -\text{sgn}(\lambda_R) \tag{16c}$$

There might exist trajectories such that some of λ_P, λ_Q, and λ_R stay zero along a time interval of finite length (singular trajectories). However, only regular extremal trajectories are considered in the present study, since there are indications that the obtained regular extremal trajectories are excellent candidates for time-optimality.[17]

IV. Parametric Studies

A. 90-Deg-RVV Family

We present next results about one family of extremal maneuvers. Each maneuver of the family can be characterized by the following initial and final states:

$$x_0 = (\alpha_{0f},\ 0 \text{ deg},\ 0 \text{ deg},\ 0,\ 0,\ 0)^T \tag{17a}$$

$$x_f = (\alpha_{0f},\ 0 \text{ deg},\ 90 \text{ deg},\ 0,\ 0,\ 0)^T \tag{17b}$$

These maneuvers are customarily called 90-deg-roll around the velocity-vector maneuvers (90-deg RVV), since one way to satisfy these conditions is with a pure velocity-vector roll with $\beta = 0$ and $\alpha = \text{const}$. Besides being rest-to-rest attitude maneuvers, for understanding the role of the dihedral-effect it is important to note that the sideslip-angle is zero at the initial and final state. The angle α_{0f} uniquely specifies a member of the family (family parameter).

A series of extremal trajectories was generated[7,8] by varying the parameter α_{0f} from 20 to 60 deg. This was done both for an aircraft with TV ($\varepsilon_t = 1$) and without TV ($\varepsilon_t = 0$). Since each of the generated extremal trajectories can be obtained numerically from any other (by varying gradually α_{0f} and/or ε_t), we say that all of these trajectories belong to a single, two-parameter extremal family.

The maneuvering time T for two 90-deg-RVV extremal subfamilies is shown in Fig. 2a. The lower (solid) line represents the TV subfamily, and the upper (dashed) line represents the subfamily of extremals without TV (only the aerodynamic surfaces used for control). The bullets and the diamonds merely represent some members of the family, and the open circles denote the points where the switching structure of the controls along the extremals changes.

In order to deduce what the global role of the dihedral effect is in the maneuvers of this 90-deg-RVV family, the following numerical experiment was performed. For each of the representative maneuvers of the family, an extremal maneuver was generated for an aircraft with no dihedral effect, by setting $C_l^0(\alpha, \beta) = 0$. Numerically, this was done by decreasing the homotopy parameter ε_l^0 from 1 to 0 for each of the representative maneuvers. An accurate measure of the global role of the dihedral effect for the maneuvers from Fig. 2a can be obtained by comparing the maneuvering time between the original extremal trajectory and the corresponding zero-$C_l^0(\alpha, \beta)$ trajectory. We adopt the relative difference in

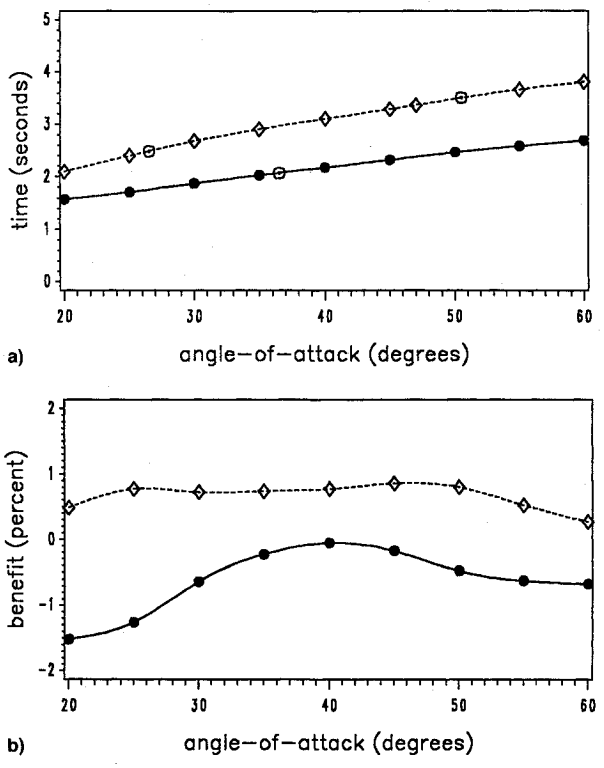

Fig. 2 90-deg RVV: a) maneuvering time vs α_{0f} and b) benefit from the dihedral effect.

time as a quantitative measure of the global role of the dihedral effect:

$$b = -\frac{T(\varepsilon_l^0 = 1) - T(\varepsilon_l^0 = 0)}{T(\varepsilon_l^0 = 1)} 100\% \tag{18}$$

Figure 2b shows the accompanying benefits $b(\alpha_{0f})$ for each of the subfamilies from Fig. 2a. Again, the solid line corresponds to the TV case, and the dashed line corresponds to the no-TV case. The dihedral-effect does not significantly alter the maneuvering time. It is interesting to note here that the no-TV subfamily takes a slight advantage from the dihedral effect, while the TV subfamily is actually adversely affected.

B. 90-Deg-Roll Family

Consider a second case wherein we present results about another family of extremal maneuvers that are also of practical interest and have tactical significance. Each maneuver of this family can be specified by the following initial and final state:

$$x_0 = (10 \text{ deg},\ 0 \text{ deg},\ 0 \text{ deg},\ 0,\ 0,\ 0)^T \tag{19a}$$

$$x_f = (\alpha_f,\ 0 \text{ deg},\ 90 \text{ deg},\ 0,\ 0,\ 0)^T \tag{19b}$$

We will refer to maneuvers of this family as 90-deg roll. Each maneuver of the family can be specified by a single constant α_f. In a similar manner as for the 90-deg-RVV family, we show in Fig. 3a the maneuvering time, both for a subfamily with (solid line) and without TV (dashed line). The no-TV subfamily ceases to exist for $\alpha_f < 35$ deg. This is related to the amount of available control power,[17] and means that singular extremals will continue this subfamily for lower angle-of-attack maneuvers. It is seen from Fig. 3b that the dihedral-effect benefit is practically zero for the no-TV subfamily, and the TV subfamily is adversely affected. Again, the change is within 1% of maneuvering time.

Thus, we conclude that for the extremal families discussed, maneuvering time is not affected significantly by the dihedral effect. We note again that these maneuvers have zero sideslip-

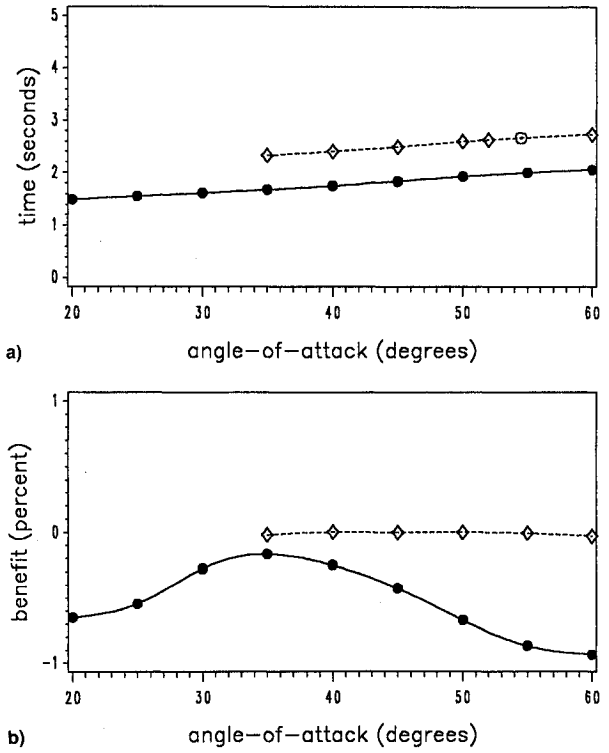

Fig. 3 90-deg roll: a) maneuvering time vs α_f and b) benefit from the dihedral effect.

angle at the initial and final state. While other extremal families are found, studies show that the extremals considered are excellent candidates for the time-optimal trajectory[8] (for the respective maneuver). Before explaining the results described above, we take a closer look at the evolution and role of various dynamical components in the mathematical model [Eqs. (7) and (8)] by describing a different fuselage-reorientation maneuver: minimum-time x^b-axis pointing.

V. Case Study: x^b-Axis Pointing Maneuver

As noted in Sec. I, the deployment of advanced weapons may simply require reorientation of the x_b axis to a specified direction. This is a less constrained problem, and thus the corresponding optimal trajectory is faster (at least no slower) than an optimal trajectory where, in addition to the orientation of the x_b axis at the terminal point, a zero sideslip-angle is required.

To gain better understanding of the minimum-time optimality, we relate the x^b-axis pointing problem to the 90-deg RVV and the 90-deg-roll problems. It is natural to use Euler angles for analysis of the x^b-axis pointing problem. The 3-2-1 sequence of Euler angles (ψ, θ, ϕ) specifies the x^b-axis orientation uniquely by the azimuth angle ψ and the elevation angle θ for all bank angles ϕ. One can establish a one-to-one correspondence between (ψ, θ, ϕ) and (α, β, μ), almost everywhere. Thus, for (α_f, $\beta_f = 0$ deg, $\mu_f = 90$ deg), the corresponding set of Euler angles is ($\psi_f = \alpha_f$, $\theta_f = 0$ deg, $\phi_f = 90$ deg). If we keep ψ_f and θ_f constant, and vary ϕ_f, we get various orientations of the aircraft, all of which have the property that the x^b axis points in one constant direction. In this manner, two families of extremal trajectories were generated, maneuvering time for which is shown by Fig. 4. The extremal family represented by the solid line is related to the 90-deg-RVV maneuver with $\alpha_{0f} = 30$ deg. The bullet represents the starting (nominal) maneuver (compare to Fig. 2a, TV case). The open circles denote the occurrence of a new control switching-sequence structure. The diamond represents the global (in ϕ) minimum-time x^b-axis pointing maneuver for this extremal family. It occurs at $\phi_f^* \approx 91.5$ deg ($\beta_f < 1$ deg).

In a similar manner, the dashed line represents an extremal family related to the 90-deg-roll maneuver with $\alpha_f = 45$ deg.

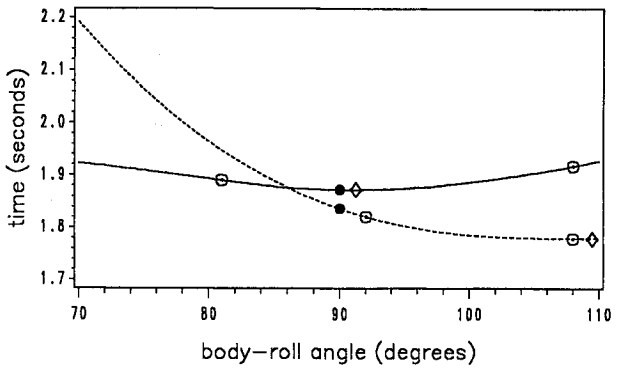

Fig. 4 Maneuvering time vs body-roll angle ϕ_f.

The global (in ϕ) minimum-time maneuver occurs at $\phi_f^* \approx 109.5$ deg. Unlike the global minimum-time maneuver of the other extremal family, here at final time the sideslip-angle is considerable ($\beta_f \approx 13$ deg).

Details about the 90-deg-roll related global minimum-time (x^b-axis pointing) maneuver are shown in Figs. 5a–5l. The horizontal axes in these plots represent the normalized time $\tau = t/T$. The evolution of the attitude angles α, β, and μ is shown in Fig. 5a, and the corresponding Euler angles in Fig. 5b. The angular-rates evolution is shown in Fig. 5c. The maneuver can be characterized as a pitch-down—pitch-up sequence, while rolling and yawing in a positive sense all the time [this can be seen best from $\alpha(\tau)$ and the angular rates]. The sideslip-angle is negative in the first portion of the trajectory, and positive in the second portion. The dihedral-effect roll-moment (Fig. 1) helps the controls accelerate the roll rate in the initial part of the trajectory, and also helps them decelerate in the terminal part, which is highly desirable since near x_f, at angles of attack close to 45 deg, the aileron effectiveness is decreased significantly. The adjoint variables λ_P, λ_Q, and λ_R, which are "responsible" for determination of the extremal controls, are shown in Fig. 5d. The scaled aerodynamic and TV controls are shown in Figs. 5e and 5f, respectively. The pitch controls δ_e and δ_v are compatible to the noted pitch-down—pitch-up sequence of motion. The differential aileron Δ_a, and δ_x, can also be understood easily: they accelerate the roll-rate in the first portion of the trajectory, and decelerate it in the second portion. The yaw controls are more difficult to understand, however, since they are positive all the time. They do not act in a negative sense in the second portion of the trajectory to decelerate the yaw-rate, as one might expect.

Figures 5g–5l show the evolution of the dynamical components in the roll, pitch, and yaw channel [Eq. (7)], and the corresponding aerodynamic components [Eq. (8)]. From Fig. 5g we see that the roll-motion is predominantly controlled by the aerodynamic component L_a [Eq. (7a)]. The gyroscopic component L_{qr} is insignificant, and the TV system generated roll-moment is also negligible. As one can see from the relative magnitude of λ_P (Fig. 5d) and Eq. (15a), the TV system exerts relatively little from the (maximum) available roll-power. The TV moment is mainly confined to the pitch and the yaw channels. Figure 5h shows the aerodynamic roll-components [Eq. (8a)]. While the damping term L_ζ opposes the initial roll-acceleration, it is quite supportive in the decelerating portion of the trajectory (as it always is). The dihedral-effect supports the aileron action most of the time, especially near the end of the trajectory where it becomes the predominant component.

In a similar manner as for the roll-channel, Figs. 5i and 5j show the dynamic pitch-components [Eq. (7b)] and the aerodynamic pitch-components [Eq. (8b)], respectively. One can see again how well all the components act in coherence (support each other) most of the time. Most significant support to the controls is due the gyroscopic term M_{rp} [Eq. (7b)]. Unlike the case with the roll channel, the TV control pitch-

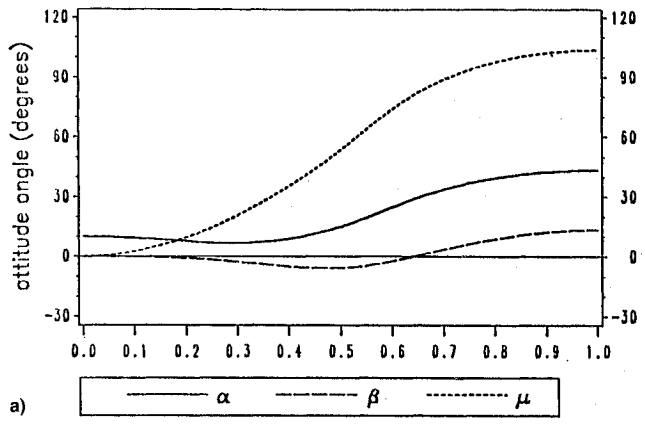

a)

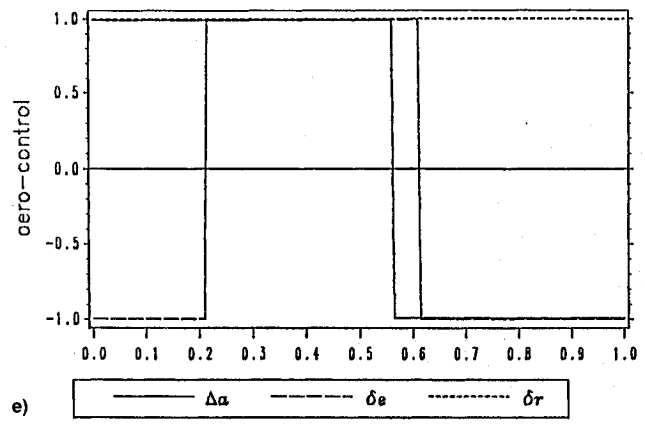

e)

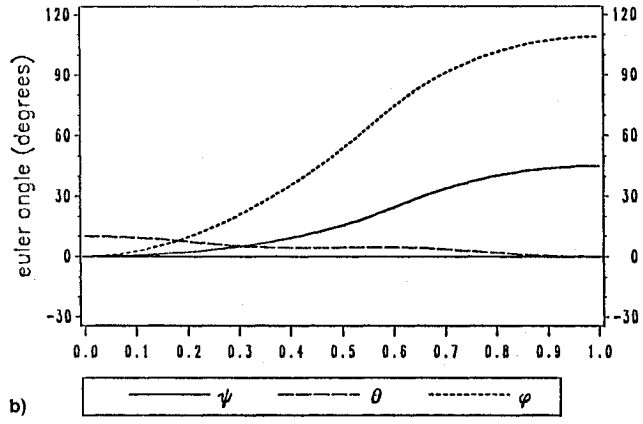

b)

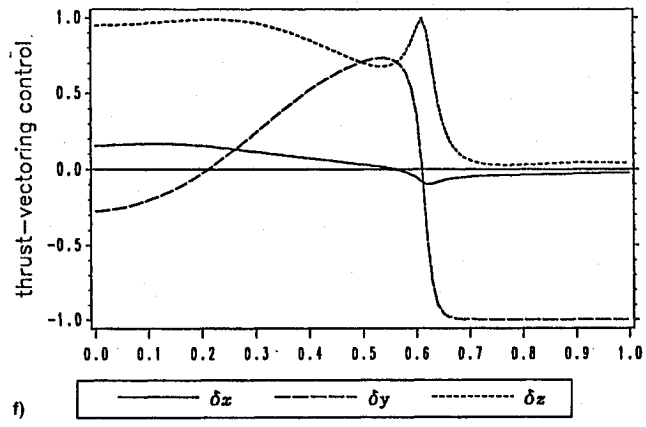

f)

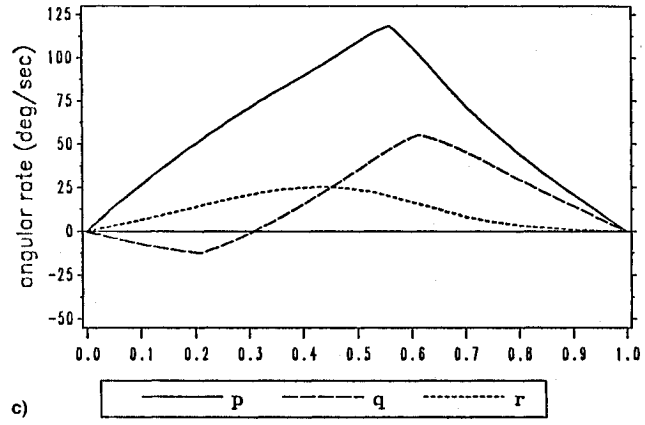

c)

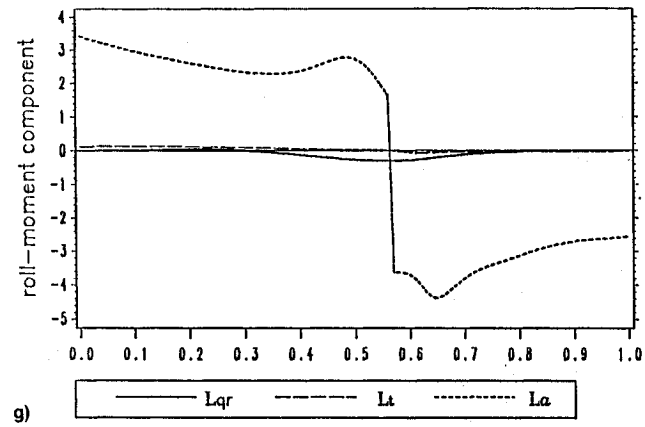

g)

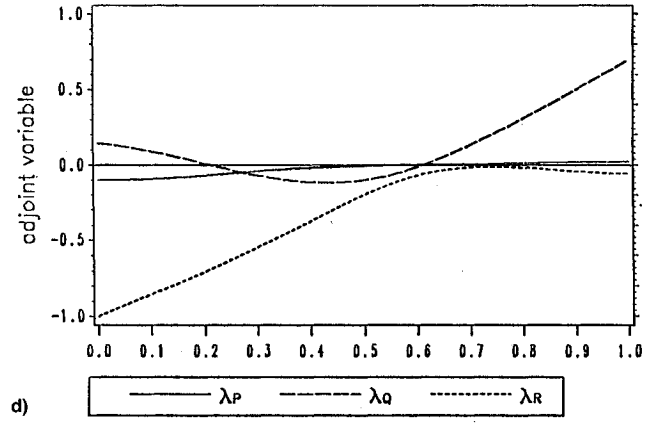

d)

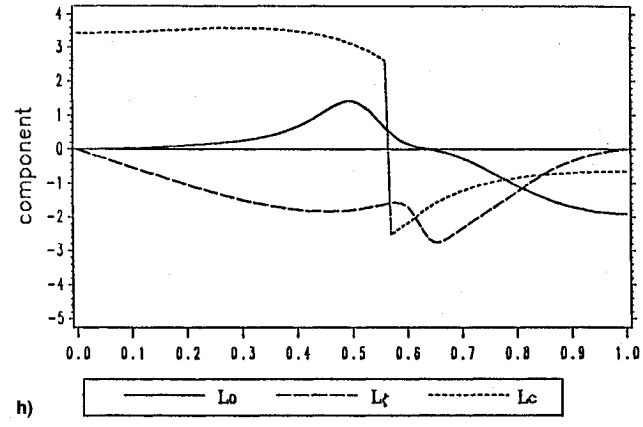

h)

Fig. 5 90-deg roll related global minimum-time maneuver details: a) angles α, β, and μ vs scaled time, b) Euler angles ψ, θ, and φ vs scaled time, c) angular rates (roll, pitch, and yaw) vs scaled time, d) angular-rate adjoint-variables vs scaled time, e) aerodynamic controls vs scaled time, f) thrust-vectoring controls vs scaled time, g) roll-dynamics components vs scaled time, h) aerodynamic roll-components vs scaled time, i) pitch-dynamics components vs scaled time, j) aerodynamic pitch-components vs scaled time, k) yaw-dynamics components vs scaled time, and l) aerodynamic yaw-components vs scaled time.

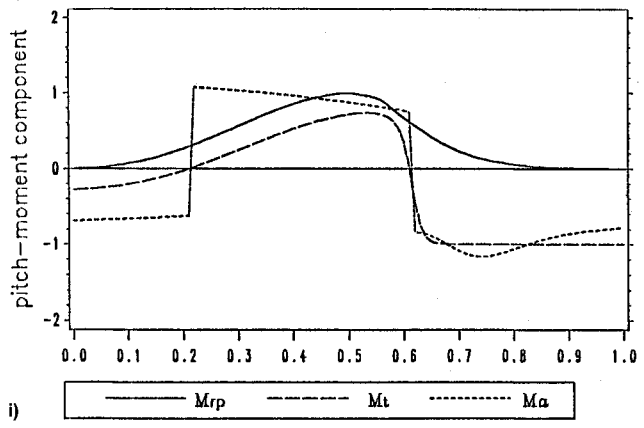

i)

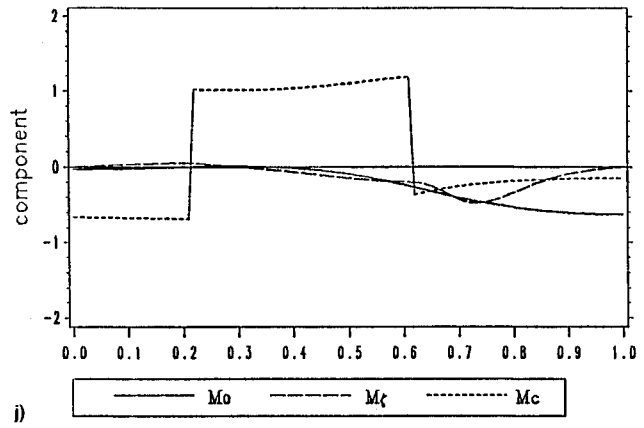

j)

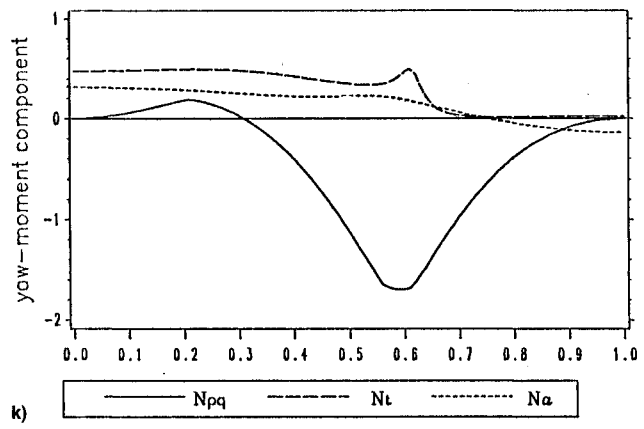

k)

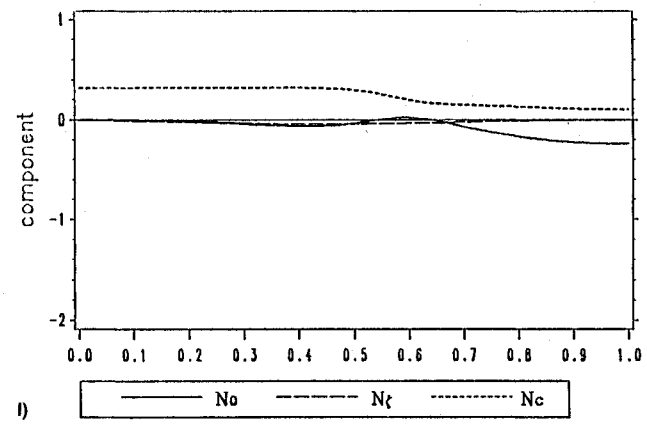

l)

Fig. 5 *(Continued)*

moment M_t and the aerodynamic pitch-moment M_α are of the same order of magnitude. Also, we should note that the static pitch-moment M_0 does not depend significantly upon β for $|\beta| < 20$ deg, and it has a supportive role near the end of the trajectory where it is actually the predominant component.

Finally, we see the yaw-channel dynamic components [Eq. (7c)] and the aerodynamic yaw-components [Eq. (8c)] in Figs. 5k and 5l, respectively. It is strikingly evident that the yaw-channel predominant component is the gyroscopic term N_{pq}. The TV term is the predominant generator of positive yaw-moment. The aerodynamic term N_α also generates a considerable amount of positive yaw-moment in the first portion of the trajectory; in the second portion it supports the negative action of the gyroscopic moment, thus helping the deceleration of the yaw rate. Now it becomes understandable why the yaw controls are positive all the time.

Due to the nature of the reorientation problem (the boundary conditions x_0 and x_f), the aircraft needs to perform a significant pitch-up motion, and also roll in a positive sense (at least most of the time). The combination of such motions unavoidably generates negative gyroscopic moment in the yaw-channel, which is substantial due to the high roll and pitch rates developed (note: the scaling on the vertical axes for the roll, pitch, and yaw channels are different). In addition, the maneuver inherently does not require a lot of yaw motion, and thus it does not need significant yaw accelerations. One can imagine a sequence of about 100-deg roll, followed by about 45-deg pitch-up, that will place the aircraft approximately in the desired x_f direction. Thus, the controls in the yaw channel are essentially used to counterbalance the negative action of the gyroscopic moment.

Actually, knowing that the described trajectory is the minimum-time one for its extremal family (represented by the dashed line in Fig. 4), it is somehow easy to accept an explanation about the evolution of various dynamical components in the course of the maneuver. In such a complex system as ours, one would expect that various "trade-offs" need be made (the concept of a tradeoff for our dynamical system can best be understood by explaining the distribution of the TV control-power in the roll, pitch, and yaw channel). In our reorientation problems, the controls guide the system in such a manner that not only is the attitude-change accomplished more effectively, but it is also supported by the other dynamical components. The initial short pitch-down sequence serves to keep the aircraft at lower angles of attack (where the aileron is more powerful) in the first half of the trajectory. In addition, this initial pitch-down motion prevents the negative gyroscopic yaw-moment from developing too early. The TV system cannot generate a substantial amount of roll moment even if used for generating roll moment only [u_ζ^0 is small, Eq. (3)]. Instead, the TV power is predominantly distributed throughout the pitch and yaw channel, in the amount needed to establish perfect balance for the maneuver being performed. How various tradeoffs are "seen" from one individual channel can best be seen from the relation (action integral)

$$\int_{\tau=0}^{\tau=1} [N_{pq}(\tau) + N_t(\tau) + N_\alpha(\tau)]\, d\tau = 0 \qquad (20)$$

which needs to hold for the yaw channel (and the roll and pitch channel, as well) since the initial and final yaw-rates are required to be the same (zero).

According to Eq. (18), the benefit in maneuvering time due to the dihedral effect for this (time-optimal) maneuver is about 6.62%, considerably more than it was the case with the extremals represented by Figs. 2 and 3. (After a maneuver such as this one is executed, and a missile fired, a subsequent recovery maneuver must take place to guide the aircraft back into a symmetric flight condition.)

VI. About the Sideslip-Angle Evolution

We elaborate now on the evolution of the sideslip-angle β in the minimum-time extremal trajectories discussed in Sec.

IV. A maneuver is specified by the attitude angles α, β, and μ at initial or final time [since we restrict ourselves to the rest-to-rest maneuvers (10)]. It is obvious that the evolution of β in the course of an extremal trajectory should essentially relate to $\beta(0)$ and $\beta(T)$, especially if these are significant in value [at least, $\beta(\tau)$ will be close to $\beta(0)$ and $\beta(T)$ in the initial and final portion of the trajectory, respectively]. When these are close or equal to zero, the $\beta(\tau)$ evolution is less obvious.

In the mathematical model, only the static moment-coefficients C_l^0, C_m^0, and C_n^0 [Eq. (5)] depend upon β (actually, C_m^0 does not depend on β, for $|\beta| < 20$ deg). Besides $\beta(0)$ and $\beta(T)$, these are the only factors that affect the evolution of β. If none of the Euler rotational equations (7) depended upon β, $\beta(\tau)$ would have been an ignorable state-variable: apart from satisfaction of $\beta(0)$ and $\beta(T)$, we would have not needed to consider β in order to understand the extremal motion.

Detailed plots, as those shown in Figs. 5a–5l, for each of the representative extremal maneuvers from Figs. 2a and 3a, show that both families can be characterized by a pitch-down—pitchup sequence, while positive roll and positive yaw being performed simultaneously (most of the time in the course of the maneuvers). Thus, for our reorientation maneuvers all of which involve high angles of attack, the α-evolution seems to be easily understandable: by lowering the angle of attack the aircraft enters a region where the aileron is more powerful and thus can generate higher roll-rates. The elevator and the rudder are also more powerful at lower angles of attack. In addition, the characteristic pitch-down—pitch-up sequence induces substantial gyroscopic moments that strongly support the action of the controls, and thus the extremal motion in general.

It remains for us to understand the evolution of the sideslip-angle, and how the β dependence of the Euler equations affects the optimization process for the minimum-time extremal fuselage-reorientation maneuvers of interest. The following numerical test provides the best explanation. For each of the representative extremal trajectories we can make a pair of plots as those in Figs. 5a–5l, for the nominal mathematical model, and for a model with no dihedral-effect [$C_l^0(\alpha, \beta) = 0$], by decreasing the homotopy parameter ε_l^0 from 1 to 0. We did this both for the TV and no-TV subfamilies. It turns out that not only are maneuvering times close, but time histories of various dynamical components are very similar [obviously, the only exception being the L_0 component, Eq. (8a)]. In particular, for each of the representative extremals, the nominal $\beta_1(\tau)$ differs from the no-dihedral $\beta_0(\tau)$ time-history very little

$$\beta_1(\tau) = \beta_0(\tau) + \Delta\beta(\tau) \tag{21}$$

where the sideslip-angles remained within 6–8 deg from zero, and the perturbations $\Delta\beta$ within at most 10–20% from the maximum β_1.

The conclusion is that the controls act to adjust the angle-of-attack time-history, as needed for efficient performance of a maneuver. The sideslip angle develops accordingly, like an "output" in the optimization process. It just happens for this extremal family that the developed sideslip-angles are low. Thus, dihedral-effect generated roll-moment has little influence upon the extremal trajectory, it merely induces a small perturbation. The sideslip-angle generated yaw-moment N_0 induces even a less significant perturbation. The above discussion elucidates that the controls do not act so as to choreograph the sideslip-angle time-history. While in some of the extremal maneuvers in Figs. 2a and 3a, the dihedral effect supports the controls in part or throughout the whole trajectory, for others it has adverse effect, partially or most of maneuvering time.

As was demonstrated by the case study, extremal maneuvers involving angles of attack around 15 deg (note the humps in Fig. 1), and those above 40 deg, and higher sideslip angles in the boundary conditions, can take more substantial advantage from the dihedral-effect.

VII. Conclusions

Studies of two broad regular extremal families of fuselage-reorientation maneuvers reveal that the dihedral effect does not play a significant role in the course of the maneuvers. Due to the very nature of the maneuvering boundary-conditions (zero sideslip-angles at initial and final time) and the character of the extremal motions, relatively low sideslip-angles develop. Thus, the dihedral-effect generated roll-moments are insignificant, compared to the available roll-control power from the aileron. The effect of the dihedral moment-coefficient in the overall optimization process is merely a slight perturbation of the extremal trajectory: maneuvering time is perturbed about 1%. A case study reveals that the dihedral effect can be quite beneficiary utilized in the course of the reorientation maneuvers (up to 10% benefit in maneuvering time) if the maneuvers involve angles of attack around 15 deg or above 40 deg (where the dihedral effect generated moments are quite substantial), and higher sideslip-angles in the boundary conditions. Such complex maneuvers might become quite attractive for future supermaneuverable aircraft.

Acknowledgments

This work was supported in part by NASA Langley Research Center, Hampton, Virginia, under Grant NAG-1-1405 and by the Air Force Office of Scientific Research under Grant F49620-92-J-0078. Special thanks are due to Jarrell R. Elliott of the Aircraft Guidance and Control Branch at the NASA Langley Research Center, whose constructive remarks motivated the creation of this article.

References

[1]Herbst, W. B., "Future Fighter Technologies," *Journal of Aircraft*, Vol. 17, No. 8, 1980, pp. 561–566.

[2]Herbst, W. B., "Dynamics of Air Combat," *Journal of Aircraft*, Vol. 20, No. 7, 1983, pp. 594–598.

[3]Well, K. H., Farber, B., and Berger, E., "Optimization of Tactical Aircraft Maneuvers Utilizing High Angles of Attack," *Journal of Guidance and Control*, Vol. 5, No. 2, 1982, pp. 131–137.

[4]Ashley, H., "On the Feasibility of Low-Speed Aircraft Maneuvers Involving Extreme Angles-of-Attack," *Journal of Fluids and Structures*, Vol. 1, July 1987, pp. 319–335.

[5]Lacey, D. W., "Air Combat Advantages from Reaction Control Systems," Society of Automotive Engineers Aerospace Congress and Exposition, TP 801177, Los Angeles, CA, Oct. 1980.

[6]Gal-Or, B., *Vectored Propulsion, Supermaneuverability and Robot Aircraft*, Springer-Verlag, New York, 1989.

[7]Bocvarov, S., "Time-Optimal Reorientation Maneuvers of an Aircraft," Ph.D. Dissertation, Aerospace and Ocean Engineering Dept., Virginia Polytechnic Inst. and State Univ., Blacksburg, VA, Aug. 1991.

[8]Bocvarov, S., Lutze, F. H., and Cliff, E. M., "Time-Optimal Reorientation Maneuvers for a Combat Aircraft," AIAA Paper 91-2709, 1991.

[9]Bundick, T., private correspondence, AGCB NASA Langley Research Center, Hampton, VA.

[10]Bryson, A. E., Jr., and Ho, Y. C., *Applied Optimal Control*, Hemisphere, New York, 1975.

[11]Pontriagin, L. S., Boltyanskii, V. G., Gamkrelidze, R. V., and Mishchenko, E. F., *The Mathematical Theory of Optimal Processes*, Interscience, New York and London, 1962.

[12]Alekseev, V. M., Tikhomirov, V. M., and Fomin, S. V., *Optimal Control*, Consultants Bureau, New York and London, 1987.

[13]Etkin, B., *Dynamics of Atmospheric Flight*, Wiley, New York, 1972, pp. 104–128.

[14]Miele, A., *Flight Mechanics*, Addison-Wesley, Reading, MA, 1962.

[15]Goldstein, H., *Classical Mechanics*, 2nd ed., Addison-Wesley, Reading, MA, 1980.

[16]Oberle, H. J., and Grimm, W., *BOUNDSCO—A Program for Numerical Solution of Optimal Control Problems*, English Translation of DFVLR-Mitt. 85-05, ICAM, Virginia Polytechnic Inst. and State Univ., Blacksburg, VA, 1988.

[17]Bocvarov, S., Cliff, E. M., and Lutze, F. H., "Some Nonintuitive Features in Time-Efficient Attitude-Maneuvers of Combat Aircraft," AIAA Paper 91-4636, 1991.